Received: 1 January 2023 | Revised: 13 April 2023 | Accepted: 13 April 2023

DOI: 10.1111/gcb.16842

Global Change Biology WILEY

RESEARCH ARTICLE

Dryness limits vegetation pace to cope with temperature change in warm regions

Bingxue Wang[1] | Weinan Chen[1,2] | Dashuan Tian[1] | Zhaolei Li[1] | Jinsong Wang[1] | Zheng Fu[1] | Yiqi Luo[3] | Shilong Piao[4] | Guirui Yu[1,2] | Shuli Niu[1,2]

[1]Key Laboratory of Ecosystem Network Observation and Modeling, Institute of Geographic Sciences and Natural Resources Research, Beijing, China

[2]College of Resources and Environment, University of Chinese Academy of Sciences, Beijing, China

[3]School of Integrative Plant Science, Cornell University, Ithaca, New York, USA

[4]Key Laboratory for Earth Surface Processes, Ministry of Education, Peking University, Beijing, China

Correspondence
Shuli Niu, Key Laboratory of Ecosystem Network Observation and Modeling, Institute of Geographic Sciences and Natural Resources Research, CAS, Beijing 100101, China.
Email: sniu@igsnrr.ac.cn

Funding information
Chinese Academy of Sciences, Grant/Award Number: 177GJH2022020BS; National Natural Science Foundation of China, Grant/Award Number: 31625006; National Key R & D Program of China, Grant/Award Number: 2022YFF0802102

Abstract

Climate change leads to increasing temperature and more extreme hot and drought events. Ecosystem capability to cope with climate warming depends on vegetation's adjusting pace with temperature change. How environmental stresses impair such a vegetation pace has not been carefully investigated. Here we show that dryness substantially dampens vegetation pace in warm regions to adjust the optimal temperature of gross primary production (GPP) (T_{opt}^{GPP}) in response to change in temperature over space and time. T_{opt}^{GPP} spatially converges to an increase of 1.01°C (95% CI: 0.97, 1.05) per 1°C increase in the yearly maximum temperature (T_{max}) across humid or cold sites worldwide (37°S–79°N) but only 0.59°C (95% CI: 0.46, 0.74) per 1°C increase in T_{max} across dry and warm sites. T_{opt}^{GPP} temporally changes by 0.81°C (95% CI: 0.75, 0.87) per 1°C interannual variation in T_{max} at humid or cold sites and 0.42°C (95% CI: 0.17, 0.66) at dry and warm sites. Regardless of the water limitation, the maximum GPP (GPP_{max}) similarly increases by 0.23 g C m^{-2} day^{-1} per 1°C increase in T_{opt}^{GPP} in either humid or dry areas. Our results indicate that the future climate warming likely stimulates vegetation productivity more substantially in humid than water-limited regions.

KEYWORDS

adaptation magnitude, carbon cycle, climate change, GPP, optimum temperature, temperature adaptation, thermal optimality, water limitation

1 | INTRODUCTION

The survival and livelihood of the earth's plants and animals are facing threats from dramatic climate changes in recent decades (Oremus et al., 2020; Thuiller et al., 2005). Although plants cannot move as freely as animals to react quickly to environmental change, the "unmovable" plants can acclimate and adapt to climate changes by altering their physiological and morphological traits, community structures, genetic composition of species, and the range of distributions to pace up with climate change (Du et al., 2017; Huang et al., 2019; Menzel et al., 2020; Niu et al., 2012). These changes are particularly vital for the biosphere because vegetation plays a key role in driving the earth's biogeochemical, water, and energy cycles, with feedback to soil, atmosphere, and climate (Franklin et al., 2016). Nevertheless, it is unclear what the vegetation's capability is to pace up with climate change and how this capability is limited by environmental stresses.

Gross primary production (GPP) of vegetation represents the most important process for both biosphere functioning and the sustainability of humanity. Future global warming is likely to have a profound impact on GPP through a temperature response of photosynthesis to temperature change. GPP generally increases with

Correspondence and requests for materials should be addressed to Bingxue Wang or Shuli Niu.

Bingxue Wang and Weinan Chen contribute equally to this work.

temperature until it reaches an optimal temperature (T_{opt}), beyond which photosynthesis declines due to the impaired Rubisco enzyme, electron transport, and stomatal closure (Sage & Kubien, 2007). The previous study has shown that T_{opt}^{GPP} varies from 8.2 to 35.8°C and increases by 0.61°C per 1°C increase in the growing season temperature across 153 eddy covariance sites over the globe (Huang et al., 2019). However, the sensitivity of T_{opt}^{GPP} to changes in temperature likely varies with water limitation as previous studies all point to a potential control of thermal adjustment of T_{opt}^{GPP} by water availability at leaf, ecosystem, and global scales (Niu et al., 2007; Quan et al., 2019). Hence, we hypothesize that T_{opt}^{GPP} of vegetation has a stronger capability to keep pace with climate change in humid regions than in dry areas.

2 | MATERIALS AND METHODS

2.1 | Calculation of optimal temperature of gross primary production and controlling factors

We used daily gross primary production (GPP) and air temperature (T_{air}) from both the LaThuile and FLUXNET2015 databases to calculate the optimal temperature of GPP (T_{opt}^{GPP}). In the two databases, all the variables related to carbon, water, and energy fluxes were quality-controlled and gap-filled by the standardized methods (Chu et al., 2017; Niu et al., 2012). Three hundred and twenty-six sites with complete whole year meteorological data (gaps <5%) were selected in this study with 1631 site-years data over large geographic areas (37°S–79°N; Figure S1). For each site-year, the daily air temperatures were binned in 1°C. The daily air temperature and GPP in each temperature bin were averaged to generate a GPP-T_{air} response curve. To avoid the noises from the diurnal pattern and the midday depression of photosynthesis, we used daily GPP and air temperature (T_{air}) instead of hourly data to generate the GPP-T_{air} response curve. Days with GPP lower than −0.5 were excluded from the data. We calculated the running mean of every three temperature bins to identify the T_{air} at the corresponding peak GPP as the optimal temperature of GPP (i.e., T_{opt}^{GPP}).

To investigate the relationships of T_{opt}^{GPP} with some key meteorological variables, we calculated the maximum temperature (T_{max}, °C), mean annual temperature (MAT, °C), and mean annual precipitation (MAP, mm year^{-1}) from the site-year data at the 326 sites. We investigated the relationships using regression tree, generalized gradient boosted model, moving window analysis, breaking point analysis, localized polynomial regression, linear regression, and linear mixed-effect model.

2.2 | Estimation of adaptation pace over space

We averaged T_{opt}^{GPP} across multiple years to investigate the spatial relationships between T_{opt}^{GPP} and the climate variables. As the relationship results from long-term adaptation to the local climate, we used the long-term climate data from the global database (WorldClim, FAO, and NOAA soil moisture data) to investigate the effects of climate factors on the optimum temperature of GPP. We first obtained MAT (°C), summer temperature (T_{summer}, °C), minimum temperature (T_{min}, °C), MAP (mm year^{-1}), summer precipitation (P_{summer}, mm year^{-1}), global solar radiation (GSR, MJ m^{-2} day^{-1}), and temperature annual range (TAR, mm year^{-1}) at each of the 326 sites from World Clim (Fick & Hijmans, 2017). Data were averaged for these variables over years 1970–2000. The warmest quarter of a year is considered summer. Aridity index (AI) was obtained from FAO dataset (https://data.apps.fao.org/map/catalog/srv/eng/catalog.search#/home), which is calculated as precipitation divided by potential evapotranspiration. Soil moisture (mm) was obtained from soil moisture data provided by the NOAA/OAR/ESRL PSD, from the Web site at https://www.esrl.noaa.gov/psd/.

A generalized gradient boosted model (Ridgeway, 2015) was used to determine the relative influence of the climate factors on T_{opt}^{GPP} with the R package "gbm". A regression tree is used to estimate the relative importance of the variable on the differences between T_{opt}^{GPP} and T_{max} with the R package "rpart" (Therneau et al., 2015). Polynomial regression was used to evaluate the relationship between GPP_{max} and T_{opt}^{GPP} across space.

The adaptation pace was defined by the spatial slope between T_{opt}^{GPP} and T_{max} across sites. Rolling window analysis (Silva, n.d.) was applied to climate variables to investigate the effects of water availability on the sensitivity of T_{opt}^{GPP} to T_{max} (i.e., $\delta T_{opt}^{GPP}/\delta T_{max}$) and the deviation of T_{opt}^{GPP} from T_{max} using a window size of 70 sites after being sorted by AI. The window size of 70 sites was selected to generate the best sensitivity and deviation. Breaking point analysis (Muggeo, 2015) was employed to identify the thresholds of AI, P_{summer} for the sensitivity of T_{opt}^{GPP} to T_{max} (i.e., $\delta T_{opt}^{GPP}/\delta T_{max}$) and the deviation from T_{opt}^{GPP} to T_{max}. We used the R package "zoo" and "segmented" for the rolling window analysis and breaking point analysis, respectively.

We grouped the 326 sites according to the obtained criteria from the moving window and breaking point analyses of AI, P_{summer}, and T_{max} (Figure S3). These sites that met all three criteria (AI < 0.98, P_{summer} < 300 mm, and T_{max} > 24.8°C) were considered dry and warm sites. All the other sites were grouped into humid or cold sites. In the cold regions, dryness does not affect vegetation pace in this study (Figure 1).

The phenology curve and the seasonal pattern of air temperature were examined by polynomial regression and localized polynomial regression (LOESS; Radhy, 2017) to examine synchrony in seasonality of temperature and GPP.

Vegetative patterns were divided into 13 plant functional types according to the International Geosphere-Biosphere Programme (IGBP) each with a corresponding number of eddy-flux sites (n): deciduous broadleaf forest (n = 42), evergreen broadleaf forest (n = 26), evergreen needle-leaf forest (n = 77), deciduous needle-leaf forest (n = 1), mixed forest, closed shrubland (CSH), opened shrubland (OSH), grassland (n = 61), cropland (n = 34), savanna (SAV, n = 12), woody savanna (WSA, n = 6), wetland (WET, n = 32), and snow and

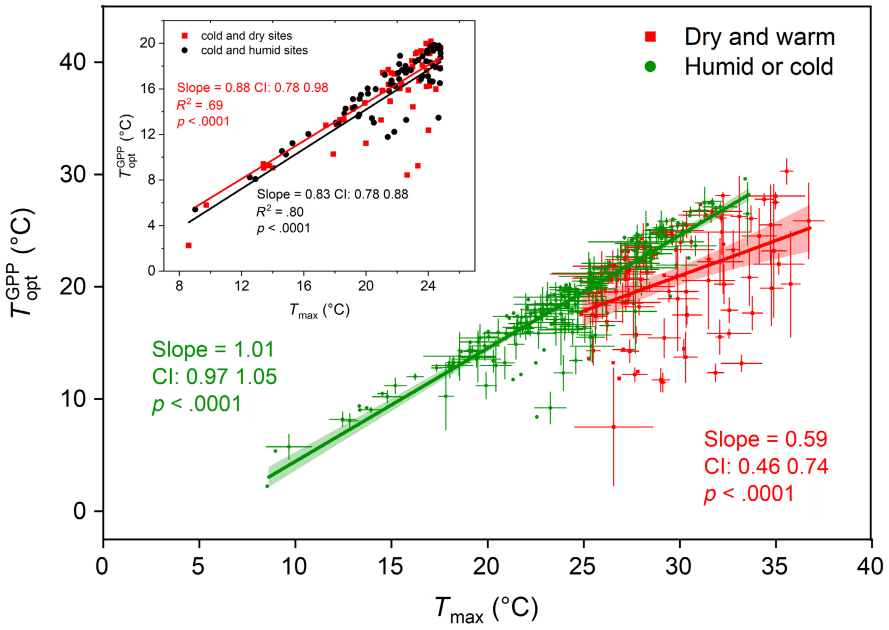

FIGURE 1 Adaptation pace of vegetation to cope with long-term temperature change. The adaptation pace was measured by the slope of a regression line of optimal gross primary production (GPP) temperature (T_{opt}^{GPP}) with yearly maximal temperature (T_{max}) across sites. Three criteria were used to separate humid or cold from dry and warm sites. The dry and warm sites were those with aridity index (AI) lower than 0.98, summer precipitation (P_{summer}) lower than 300 mm, and $T_{max} > 24.8$. All the other sites belonged to the group of humid or cold sites (see Section 2 for description of the criteria). Error bars indicate the standard deviation. The shaded area is the 95% confidence interval of the regression lines. The adaptation pace was 1.01 (95% CI: 0.97, 1.05) across the humid FLUXNET sites (blue dot) and 0.59 (95% CI: 0.46, 0.74) across the dry and warm sites (pink dot). Inset shows the adaptation pace of T_{opt}^{GPP} in cold and dry sites ($T_{max} < 24.8$°C, AI < 0.98, and $P_{summer} < 300$ mm) versus cold and humid sites ($T_{max} < 24.8$°C, AI > 0.98, or $P_{summer} > 300$ mm). [Colour figure can be viewed at wileyonlinelibrary.com]

ice ($n = 1$). For improving the power of statistical analysis, CSH ($n = 8$) and OSH ($n = 14$) were merged into shrubland (SH); SAV and WSA were merged into SAV. The global distribution of these vegetation types was derived from MODIS (MOD12Q1 Land Cover Science Data Product) at a spatial resolution of 1 km. These vegetation types were analyzed for their differences in the adaptation pace of T_{opt}^{GPP} to T_{max} (i.e., $\delta T_{opt}^{GPP}/\delta T_{max}$) based on linear regression and analysis of variance. Then we calculated the difference between T_{max} and T_{opt}^{GPP} (T_{dev}) and used linear regression to assess the sensitivity of T_{dev} to AI and summer precipitation for each vegetation type.

2.3 | Estimation of acclimation pace

We calculated the temporal slope between T_{opt}^{GPP} and T_{max} within a site as the acclimation pace. Sites with more than 6 years of data were used to evaluate the acclimation of T_{opt}^{GPP} to T_{max} across years. The standard deviation of the acclimation pace stabilized when data from sites with less than 6 years data were excluded. There were a total of 86 sites with data of 6 years or longer. According to the three criteria on AI, P_{summer}, and T_{max}, there were 45 sites and 539 site-year data in the humid or cold group, and 41 sites and 431 site-year data in the dry and warm group for the linear mixed-effects model analysis. We modeled the temporal relationships with linear mixed-effects models by using the R package "nlme" (Pinheiro et al., 2014). T_{max} and MAP were treated as fixed effects. Sites were treated as a random effect, allowing both the slopes and intercepts to vary between sites if supported by model selection. We allowed intercepts to vary among sites for the analysis of the acclimation of T_{opt}^{GPP} to T_{max} in humid or cold sites because the lines did not converge. For all other analyses, we allowed both intercepts and slopes to vary among sites. The temporal relationship between GPP_{max} and T_{opt}^{GPP} was modeled with a linear mixed-effects model as well. We analyzed the influence of all possible drivers for the acclimation pace using the "glmulti" package in R (Calcagno, 2013). The regression tree was used to model the acclimation pace using the R package "rpart" (Therneau et al., 2015). We then predicted global T_{opt}^{GPP} and the acclimation pace using the regression tree model.

All statistical analyses were performed using R ×64 3.3.1 for Windows.

Graphs were constructed using package "ggplot2".

3 | RESULTS AND DISCUSSION

We analyzed GPP data from 326 FLUXNET eddy covariance sites from 37°S to 79°N over the globe (Figure S1) to quantify the sensitivity of T_{opt}^{GPP} to change in air temperature. We averaged T_{opt}^{GPP} over years at each site to calculate the spatial slope between T_{opt}^{GPP} and air temperature across sites. The slope represents the vegetation's capability to pace with temperature change via long-term shifts in community structures, species genetic composition, and the range of distributions (i.e., the adaptation pace hereinafter). T_{opt}^{GPP} ranged from 2.3 to 30.3°C

across the 326 FLUXNET sites (Figure S2). T_{opt}^{GPP} was significantly correlated with the maximum temperature (T_{max}) with a slope of 0.79°C per °C across the 326 sites (Figure S2a). There was an envelope line T_{opt}^{GPP} in parallel to the 1:1 line with T_{max} (Figure S2a,b). Among several climate variables, T_{max} was the most important one in determining T_{opt}^{GPP} (Figure S2c). A frequency distribution shows that the T_{opt}^{GPP} was lower than T_{max} with a mode of 4.6°C (Figure S2d). The deviation between T_{opt}^{GPP} and T_{max} was related to water availability such as precipitation of summer (P_{summer}) and AI (Figure S2d inset).

To test the hypothesis that water limitation lowers the adaptation pace (i.e., vegetation pace to cope with long-term temperature change via thermal adaptation), we first established three criteria to delineate dry from humid sites. The three criteria were (1) the sensitivity of T_{opt}^{GPP} to the spatial variation in T_{max} (i.e., $\delta T_{opt}^{GPP}/\delta T_{max}$) as related to AI and (2) summer precipitation (P_{summer}), and (3) the influence of AI on the deviation of (T_{max}-T_{opt}^{GPP}) as dependent on temperature using the moving window analysis and breaking point analysis (see Section 2; Table S1; Figure S3). The estimated sensitivity $\delta T_{opt}^{GPP}/\delta T_{max}$ was about 1.0°C/°C when the averaged AI >0.98 (95% CI: 0.95, 1) but gradually decreased to 0.65°C/°C as AI decreased from 0.98 to 0.40 (Figure S3a). The sensitivity increased with increasing summer precipitation when it was less than 300 mm and stayed around 1 when the summer precipitation was larger than 300 mm (Figure S3b). Moreover, AI only affected T_{opt}^{GPP} at those sites with T_{max} larger than 24.8°C (95% CI: 24.3, 25.2), below which water stresses did not influence the adaptation pace (Figure S3c).

We grouped the 326 sites according to the obtained criteria from the moving window and breaking point analyses of AI, P_{summer}, and T_{max}. These sites that met all three criteria (AI < 0.98, P_{summer} < 300 mm, and T_{max} > 24.8°C) were considered dry and warm sites. All the other sites were grouped into humid or cold sites. Across the humid or cold sites, a regression line $T_{opt}^{GPP} = 1.01T_{max} - 5.63$ well represented the observations ($R^2 = .87$, $p < .001$; Figure 1). the adaptation pace was 1.01°C/°C across the humid or cold sites. In contrast, the adaptation pace was 0.59°C/°C across the dry and warm sites. The variation of T_{opt}^{GPP} among the humid or cold sites was well explained by T_{max} (94%), slightly affected by summer precipitation (0.4%), but not by vegetation types or their interactions (Table S2). Across the dry and warm sites, T_{max} alone only explained 28% of the variation in T_{opt}^{GPP} ($p < .001$). Incorporating summer precipitation, vegetation types, and these statistically significant interactions into the regression equation increased the explained variance in T_{opt}^{GPP} to 66% (Table S2). Vegetation types not only directly but also interactively influenced T_{opt}^{GPP} with summer precipitation at dry and warm sites ($p < .001$, Table S2). It implies that vegetation types in dry and warm sites had different strategies (i.e., varying adaptation paces) to cope with temperature change in water-limiting sites (Figure S4a). The WET ecosystems, for example, had an adaptation pace of about 1°C/°C regardless of AI or P_{summer} (Figure S4). While the adaptation pace of savanna was not significantly different from zero (Figure S4a), the deviation of T_{opt}^{GPP} from T_{max} significantly varied with change in AI or P_{summer} in shrub and savanna (Figure S4b,c). Our finding is consistent with a global analysis of stomatal behavior among plant functional types according to the marginal carbon cost of water use (Lin et al., 2015).

We also analyzed the temporal relationship between T_{opt}^{GPP} and air temperature at individual sites to represent short-term adjustment in physiological and morphological processes (i.e., the acclimation pace hereinafter) at the sites where at least 6 years of data were available. To test the hypothesis that dryness reduces the acclimation pace of T_{opt}^{GPP}, we compared the temporal slope of T_{opt}^{GPP} regression with T_{max} between humid or cold sites versus dry and warm sites. The temporal slope between T_{opt}^{GPP} and T_{max}, on average, was 0.81°C (95% CI: 0.75, 0.87, Figure 2a) for humid or cold sites. The 95% confidence

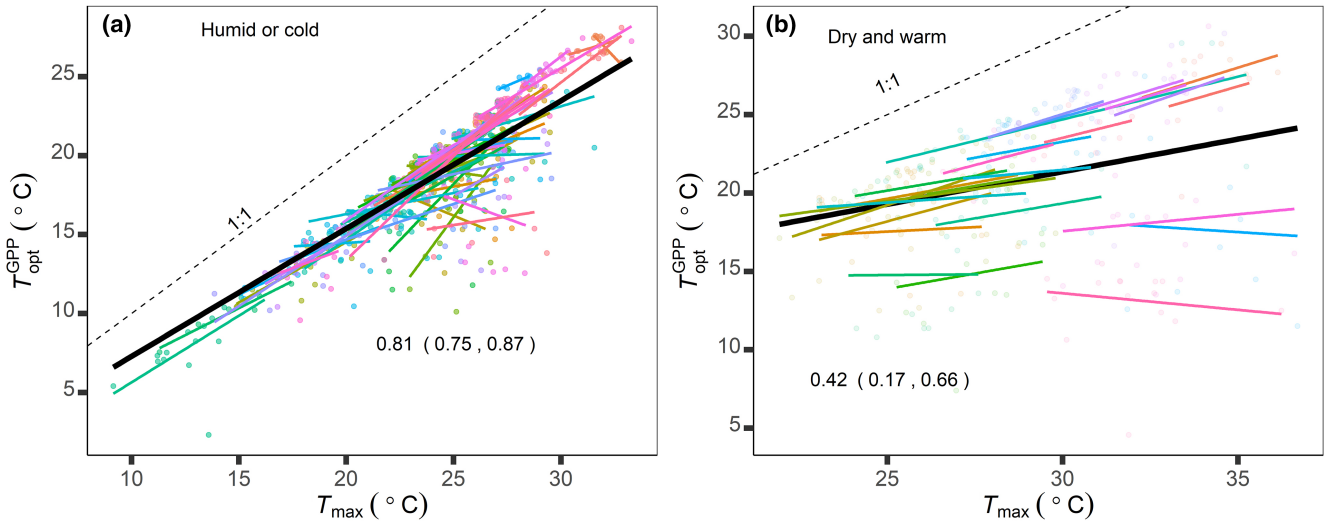

FIGURE 2 Acclimation pace of vegetation to cope with interannual temperature change. The acclimation pace was measured by the slope of the regression between optimal gross primary production (GPP) temperature (T_{opt}^{GPP}) and the maximal temperature (T_{max}) across years at individual sites (thin color lines). Each dot represents one site-year data. Data from the same site were in the same color. The thick black line was the fixed-effect linear regression slope between sites (i.e., the acclimation pace across sites) estimated from the linear mixed-effects model. It was 0.81 (95% CI: 0.75, 0.87) for the humid or cold sites (a) and 0.42 (95% CI: 0.17, 0.66) for the dry and warm sites (b). The separation of the humid or cold sites from dry and warm sites was based on the three criteria as described in Figure 1. [Colour figure can be viewed at wileyonlinelibrary.com]

interval did not include 1, indicating T_{opt}^{GPP} does not fully acclimate to T_{max}, even if water is not limiting. Water limitation reduced the acclimation pace to 0.42°C (95% CI: 0.17, 0.66, Figure 2b) in dry and warm sites. Dryness-induced decreases in the acclimation pace partly resulted from the peak photosynthesis that occurred months before the seasonal peak temperature (Figure S5), which was also observed in dry grasslands in China (Yang et al., 2019). The phenology of vegetation photosynthesis would be likely advanced more by warming-induced drought in the future, especially for those dry ecosystems (Park et al., 2019; Wang et al., 2020; Xu et al., 2016; Yang et al., 2019).

T_{opt}^{GPP} showed a higher adjustment pace to T_{max} across space than over time either at humid or dry and warm sites. The adaptation pace reflects the vegetation's capability to cope with a changing environment via long-term changes in genetic materials, reorganization of community structures, and shifts in distributions over generations (Smith & Dukes, 2013). The acclimation pace operates at a yearly and monthly scale when physiological and morphological adjustments happen without these long-term mechanisms (Smith & Dukes, 2013). Nevertheless, the lowered pace via thermal acclimation was relatively moderate (i.e., ~20% at humid or cold sites and 30% at dry and warm sites) in comparison with that via thermal adaptation.

We developed a regression tree model and multivariate regression to explain the variation in T_{opt}^{GPP} across a large geographic area (Figure S6). While they have comparable explanatory power, we used the regression tree model to predict a global average T_{opt}^{GPP}, which was averaged at 18.8 ± 7.1°C under current climate conditions (Figure 3a). It was considerably lower than a previously reported value of 23 ± 7.8°C (Huang et al., 2019), likely due to the incorporation of P_{summer}, AI, and vegetation types to constrain T_{opt}^{GPP} in our study.

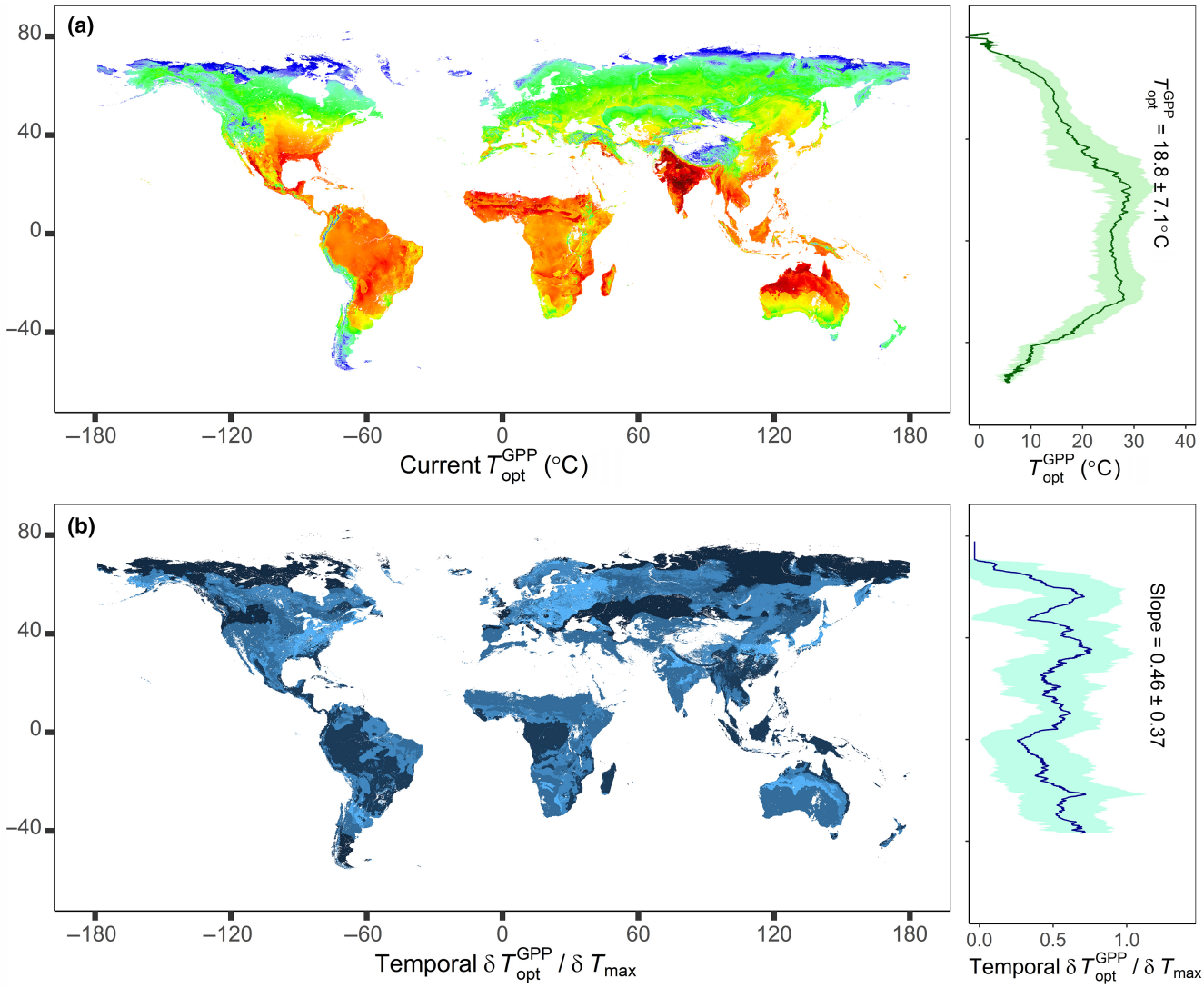

FIGURE 3 Global distributions of optimum gross primary production (GPP) temperature and acclimation pace. Spatial distribution of optimum GPP temperature (T_{opt}^{GPP}) over the globe (a) and T_{opt}^{GPP} averaged by latitude (b). Spatial distribution of acclimation pace (c) and acclimation pace averaged by latitude (d). Error bars indicate ±SD. The spatial distributions of optimum GPP temperature and the acclimation pace both were predicted by their respective regression tree models (see Section 2). [Colour figure can be viewed at wileyonlinelibrary.com]

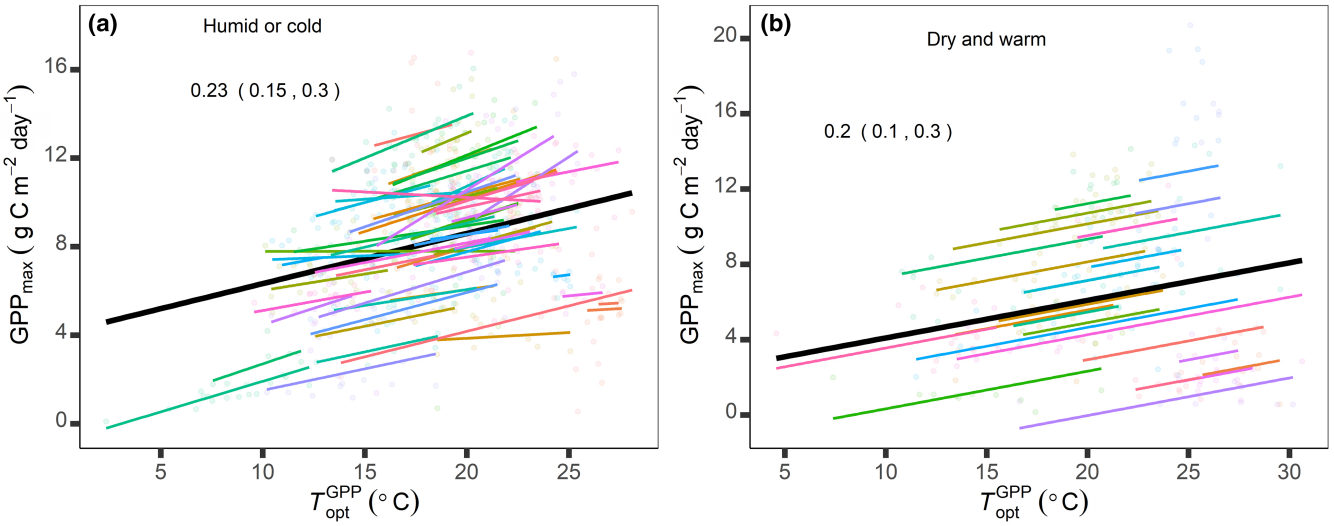

FIGURE 4 Change in vegetation carbon uptake due to shifts in optimal gross primary production (GPP) temperature. The regression slope between maximum GPP (GPP_{max}) and optimum GPP temperature (T_{opt}^{GPP}) across all the sites and years was 0.23 (95% CI: 0.15, 0.30) for the humid or cold sites and 0.20 (95% CI: 0.10, 0.30) for the dry and warm sites. [Colour figure can be viewed at wileyonlinelibrary.com]

The acclimation pace over years across widely different sites is primarily influenced by the deviation of T_{opt}^{GPP} from T_{max}, which explained only 9% of the variation in acclimation pace (Figure S7a,b). The acclimation pace had no significant difference among the vegetation types ($p < .05$, Figure S7c) although the AI of vegetation types significantly differed among them ($p < .001$, Figure S7d). The acclimation pace varied most within SH and savanna, the vegetation types in dry regions. We developed a regression tree model to predict acclimation pace ($R^2 = .34$, Figure S7e). The model predicted the averaged global acclimation pace to be 0.46 ± 0.37 without a clear trend across the latitudinal gradient (Figure 3b).

To further investigate how shifts in T_{opt}^{GPP} would influence ecosystem carbon cycle, we analyzed change in GPP_{max} in association with change in T_{opt}^{GPP}. GPP_{max} tended to be higher in years with higher T_{opt}^{GPP}, with a slope of 0.23 (95% CI: 0.15, 0.30, Figure 4a) at the humid or cold sites and 0.20 (95% CI: 0.10, 0.30) at the dry and warm sites (Figure 4b). This suggests that water limitation does not significantly affect the temporal slope between GPP_{max} and T_{opt}^{GPP}. We merged data from both humid and dry sites for regression analysis and found that 1°C increase in T_{opt}^{GPP} led to an increase in GPP_{max} by 0.23 g $C\,m^{-2}\,day^{-1}$ (95% CI: 0.16, 0.30). As the vegetation adjustment pace via adaptation and acclimation was slower at dry and warm than the other sites, humid or cold regions would gain more climate warming-induced benefit in carbon uptake via vegetation adjustment than dry and warm regions in the future.

Results from this study offer the potential to improve the prediction of vegetation carbon uptake under climate change. Leaf-level knowledge has been incorporated into earth system models (ESMs) to represent thermal acclimation and adaptation (Kattge & Knorr, 2007; Kumarathunge et al., 2019; Sendall et al., 2015; Yamori et al., 2014). The leaf-level modeling approach likely overestimates the thermal adjustment as the ecosystem-scale T_{opt} was consistently lower than the leaf-level T_{opt} (Huang et al., 2018). It would be relatively easy to implement the revealed adaptation pace of T_{opt}^{GPP} in this study into ESMs, especially in humid regions where T_{opt}^{GPP} closely tracks the maximum air temperature. It may require some types of machine learning models to simulate the adaptation and acclimation paces in dry regions as multiple factors and processes influence them as shown by this study.

This study revealed that vegetation cannot well adjust its optimal temperature in dry and warm regions but can pace up very well with temperature change in other regions. Although plant species and vegetation distributions cannot shift fast enough to keep up with temperature change under global warming, ecosystem carbon uptake, a key function of vegetation, can completely pace up with temperature change over space in humid or cold regions through a combination of long-term shifts in community structures, species genetic composition, and the range of distributions (i.e., the adaptation pace; Burrows et al., 2011; Huang et al., 2017; Loarie et al., 2009; Penuelas et al., 2013; Zellweger et al., 2020). Even with a given community structure in humid or cold regions, the acclimation pace can almost match temperature change over years (i.e., 0.81°C T_{opt}^{GPP} over 1°C T_{max}). However, the pace was severely dampened in the dry and warm regions either via adaptation or acclimation. These findings help understand the influence of climate change on carbon uptake over the globe. When vegetation paces up to rising temperature by shifting the temperature optima upward, ecosystem carbon uptake increases proportionally. The reduced pace under dry and warm conditions highlights the great vulnerability of large, extensive areas of arid and semiarid regions to a warming and drier future (Huang et al., 2015; Lian et al., 2021).

AUTHOR CONTRIBUTIONS

Bingxue Wang collected and analyzed the data, created graphs, and drafted the manuscript. Weinan Chen collected data from FluxNet and estimated the optimum temperature and maximum gross primary production. Shuli Niu conceived the idea and supervised the work. Dashuan

Tian, Zhaolei Li, Jinsong Wang, Zheng Fu, Yiqi Luo, Shilong Piao, and Guirui Yu contributed to data analysis, interpretation, and wording. All authors commented on and approved the final manuscript.

ACKNOWLEDGMENTS

This work is financially supported by the National Natural Science Foundation of China (31625006), National Key R & D Program of China (2022YFF0802102), and International Partnership Program of Chinese Academy of Science (177GJH2022020BS). We used the eddy covariance data of the FLUXNET community by the following networks: AmeriFlux (US Department of Energy, Biological and Environmental Research, Terrestrial Carbon Program [DE-FG02-04ER63917 and DE-FG02-04ER63911]), AisaFlux (supported by Asia-Pacific Network for Global Change Research), GHG-Europe, Fluxnet-Canada Research Network and Canadian Carbon Program (supported by CFCAS, NSERC, BIOCAP, Environment Canada, and NRCan), BERMS (Boreal Ecosystem Research and Monitoring Sites), KoFlux, LBA, ChinaFlux, JapanFlux, NECC, OzFlux, USCCC, European Fluxes Database (Current database for CarboAfrica, CarboEurope, CarboItaly, EuroFlux, GreenGrass, IMECC, and TCOS Siberia), ICOS (Integrated Carbon Observation System), IWFLUX (Inland Water Greenhouse Gas FLUX), MexFlux, RusFluxNet, Swiss Fluxnet, TCOS Siberia (Terrestrial Carbon Observation System Siberia), and Urban Fluxnet. We appreciate the financial support for the eddy covariance data.

CONFLICT OF INTEREST STATEMENT

The authors declare no competing interests.

DATA AVAILABILITY STATEMENT

All FLUXNET data can be downloaded at: https://fluxnet.org/. Meteorological data at each of the 326 sites were obtained from World Clim (http://worldclim.org/). Aridity index (AI) was obtained from FAO dataset (https://data.apps.fao.org/map/catalog/srv/eng/catalog.search#/home). Soil moisture (mm) was obtained from soil moisture data provided by the NOAA/OAR/ESRL PSD, Boulder, Colorado, USA, from the Web site at https://www.esrl.noaa.gov/psd/. The calculated T_{opt}^{GPP} and spatial acclimation pace of T_{opt}^{GPP} are available at https://figshare.com/articles/dataset/Sites_Topt_xlsx/23537826.

ORCID

Weinan Chen https://orcid.org/0000-0003-0227-4454
Dashuan Tian https://orcid.org/0000-0001-8023-1180
Jinsong Wang https://orcid.org/0000-0002-3425-7387
Zheng Fu https://orcid.org/0000-0001-7627-8824
Yiqi Luo https://orcid.org/0000-0002-4556-0218
Shilong Piao https://orcid.org/0000-0001-8057-2292
Guirui Yu https://orcid.org/0000-0002-1859-8966
Shuli Niu https://orcid.org/0000-0002-2394-2864

REFERENCES

Burrows, M. T., Schoeman, D. S., Buckley, L. B., Moore, P., Poloczanska, E. S., Brander, K. M., Brown, C., Bruno, J. F., Duarte, C. M., Halpern, B. S., Holding, J., Kappel, C. V., Kiessling, W., O'Connor, M. I., Pandolfi, J. M., Parmesan, C., Schwing, F. B., Sydeman, W. J., & Richardson, A. J. (2011). The pace of shifting climate in marine and terrestrial ecosystems. *Science*, *334*(6056), 652–655. https://doi.org/10.1126/science.1210288

Calcagno, V. (2013). glmulti: Model selection and multimodel inference made easy. https://cran.r-project.org/web/packages/glmulti/glmulti.pdf

Chu, H., Baldocchi, D. D., John, R., Wolf, S., & Reichstein, M. (2017). Fluxes all of the time? A primer on the temporal representativeness of FLUXNET. *Journal of Geophysical Research: Biogeosciences*, *122*(2), 289–307. https://doi.org/10.1002/2016JG003576

Du, Y.-P., Bi, Y., Zhang, M.-F., Yang, F.-P., Jia, G.-X., & Zhang, X.-H. (2017). Genome size diversity in *Lilium* (Liliaceae) is correlated with karyotype and environmental traits. *Frontiers in Plant Science*, *8*, 1303. https://doi.org/10.3389/fpls.2017.01303

Fick, S. E., & Hijmans, R. J. (2017). WorldClim 2: New 1-km spatial resolution climate surfaces for global land areas. *International Journal of Climatology*, *37*(12), 4302–4315. https://doi.org/10.1002/joc.5086

Franklin, J., Serra-Diaz, J. M., Syphard, A. D., & Regan, H. M. (2016). Global change and terrestrial plant community dynamics. *Proceedings of the National Academy of Sciences of the United States of America*, *113*(14), 3725–3734. https://doi.org/10.1073/pnas.1519911113

Huang, J., Yu, H., Guan, X., Wang, G., & Guo, R. (2015). Accelerated dryland expansion under climate change. *Nature Climate Change*, *6*(2), 166–171. https://doi.org/10.1038/nclimate2837

Huang, K., Xia, J., Wang, Y., Ahlström, A., Chen, J., Cook, R. B., Cui, E., Fang, Y., Fisher, J. B., Huntzinger, D. N., Li, Z., Michalak, A. M., Qiao, Y., Schaefer, K., Schwalm, C., Wang, J., Wei, Y., Xu, X., Yan, L., … Luo, Y. (2018). Enhanced peak growth of global vegetation and its key mechanisms. *Nature Ecology & Evolution*, *2*, 1897–1905. https://doi.org/10.1038/s41559-018-0714-0

Huang, M., Piao, S., Ciais, P., Penuelas, J., Wang, X., Keenan, T. F., Peng, S., Berry, J. A., Wang, K., Mao, J., Alkama, R., Cescatti, A., Cuntz, M., De Deurwaerder, H., Gao, M., He, Y., Liu, Y., Luo, Y., Myneni, R. B., … Janssens, I. A. (2019). Air temperature optima of vegetation productivity across global biomes. *Nature Ecology & Evolution*, *3*(5), 772–779. https://doi.org/10.1038/s41559-019-0838-x

Huang, M., Piao, S., Janssens, I. A., Zhu, Z., Wang, T., Wu, D., Ciais, P., Myneni, R. B., Peaucelle, M., Peng, S., Yang, H., & Penuelas, J. (2017). Velocity of change in vegetation productivity over northern high latitudes. *Nature Ecology & Evolution*, *1*(11), 1649–1654. https://doi.org/10.1038/s41559-017-0328-y

Kattge, J., & Knorr, W. (2007). Temperature acclimation in a biochemical model of photosynthesis: A reanalysis of data from 36 species. *Plant, Cell & Environment*, *30*(9), 1176–1190. https://doi.org/10.1111/j.1365-3040.2007.01690.x

Kumarathunge, D. P., Medlyn, B. E., Drake, J. E., Tjoelker, M. G., Aspinwall, M. J., Battaglia, M., Cano, F. J., Carter, K. R., Cavaleri, M. A., Cernusak, L. A., Chambers, J. Q., Crous, K. Y., De Kauwe, M. G., Dillaway, D. N., Dreyer, E., Ellsworth, D. S., Ghannoum, O., Han, Q., Hikosaka, K., … Way, D. A. (2019). Acclimation and adaptation components of the temperature dependence of plant photosynthesis at the global scale. *New Phytologist*, *222*(2), 768–784. https://doi.org/10.1111/nph.15668

Lian, X., Piao, S., Chen, A., Huntingford, C., Fu, B., Li, L. Z. X., Huang, J., Sheffield, J., Berg, A. M., Keenan, T. F., McVicar, T. R., Wada, Y., Wang, X., Wang, T., Yang, Y., & Roderick, M. L. (2021). Multifaceted characteristics of dryland aridity changes in a warming world. *Nature Reviews Earth & Environment*, *2*(4), 232–250. https://doi.org/10.1038/s43017-021-00144-0

Lin, Y.-S., Medlyn, B., Duursma, R., Prentice, I., Wang, H., Baig, S., Eamus, D., Resco de Dios, V., Mitchell, P., Ellsworth, D., Op de Beeck, M., Wallin, G., Uddling, J., Tarvainen, L., Linderson, M.-L., Cernusak, L., Nippert, J., Ocheltree, T., Tissue, D., & Wingate, L. (2015). Optimal

stomatal behaviour around the world. *Nature Climate Change*, *5*, 459–464. https://doi.org/10.1038/nclimate2550

Loarie, S. R., Duffy, P. B., Hamilton, H., Asner, G. P., Field, C. B., & Ackerly, D. D. (2009). The velocity of climate change. *Nature*, *462*(7276), 1052–1055. https://doi.org/10.1038/nature08649

Menzel, A., Yuan, Y., Matiu, M., Sparks, T., Scheifinger, H., Gehrig, R., & Estrella, N. (2020). Climate change fingerprints in recent European plant phenology. *Global Change Biology*, *26*(4), 2599–2612. https://doi.org/10.1111/gcb.15000

Muggeo, V. (2015). Regression models with breakpoints/changepoints estimation.

Niu, S., Luo, Y., Fei, S., Yuan, W., Schimel, D., Law, B. E., Ammann, C., Altaf Arain, M., Arneth, A., Aubinet, M., Barr, A., Beringer, J., Bernhofer, C., Andrew Black, T., Buchmann, N., Cescatti, A., Chen, J., Davis, K. J., Dellwik, E., … Zhou, X. (2012). Thermal optimality of net ecosystem exchange of carbon dioxide and underlying mechanisms. *New Phytologist*, *194*(3), 775–783. https://doi.org/10.1111/j.1469-8137.2012.04095.x

Niu, S., Wu, M., Han, Y., Xia, J., Li, L., & Wan, S. (2007). Water-mediated responses of ecosystem carbon fluxes to climatic change in a temperate steppe. *New Phytologist*, *177*(1), 209–219. https://doi.org/10.1111/j.1469-8137.2007.02237.x

Oremus, K. L., Bone, J., Costello, C., García Molinos, J., Lee, A., Mangin, T., & Salzman, J. (2020). Governance challenges for tropical nations losing fish species due to climate change. *Nature Sustainability*, *3*(4), 277–280. https://doi.org/10.1038/s41893-020-0476-y

Park, T., Chen, C., Macias-Fauria, M., Tommervik, H., Choi, S., Winkler, A., Bhatt, U. S., Walker, D. A., Piao, S., Brovkin, V., Nemani, R. R., & Myneni, R. B. (2019). Changes in timing of seasonal peak photosynthetic activity in northern ecosystems. *Global Change Biology*, *25*(7), 2382–2395. https://doi.org/10.1111/gcb.14638

Penuelas, J., Sardans, J., Estiarte, M., Ogaya, R., Carnicer, J., Coll, M., Barbeta, A., Rivas-Ubach, A., Llusia, J., Garbulsky, M., Filella, I., & Jump, A. S. (2013). Evidence of current impact of climate change on life: A walk from genes to the biosphere. *Global Change Biology*, *19*(8), 2303–2338. https://doi.org/10.1111/gcb.12143

Pinheiro, J., Bates, D., Debroy, S., & Sarkar, D. (2014). R Core Team: nlme: Linear and nonlinear mixed effects models.

Quan, Q., Tian, D., Luo, Y., Zhang, F., Crowther, T. W., Zhu, K., Chen, H. Y., Zhou, Q., & Niu, S. (2019). Water scaling of ecosystem carbon cycle feedback to, water scaling of ecosystem carbon cycle feedback to climate warming climate warming. *Science Advances*, *5*, eaav1131. https://doi.org/10.1126/sciadv.aav1131

Radhy, Z. H. (2017). The technique of Robust—Loess in regression analysis.

Ridgeway, G. (2015). gbm: Generalized boosted regression models.

Sage, R. F., & Kubien, D. S. (2007). The temperature response of C3 and C4 photosynthesis. *Plant Cell and Environment*, *30*(9), 1086–1106. https://doi.org/10.1111/j.1365-3040.2007.01682.x

Sendall, K. M., Reich, P. B., Zhao, C., Jihua, H., Wei, X. O., Stefanski, A., Rice, K., Rich, R. L., & Montgomery, R. A. (2015). Acclimation of photosynthetic temperature optima of temperate and boreal tree species in response to experimental forest warming. *Global Change Biology*, *21*(3), 1342–1357. https://doi.org/10.1111/gcb.12781

Silva, R. R. (n.d.). [R] moving-window analysis.

Smith, N. G., & Dukes, J. S. (2013). Plant respiration and photosynthesis in global-scale models: Incorporating acclimation to temperature and CO_2. *Global Change Biology*, *19*(1), 45–63. https://doi.org/10.1111/j.1365-2486.2012.02797.x

Therneau, T., Atkinson, B., & Ripley, B. (2015). rpart: recursive partitioning for classification, regression and survival trees.

Thuiller, W., Lavorel, S., Araujo, M. B., Sykes, M. T., & Prentice, I. C. (2005). Climate change threats to plant diversity in Europe. *Proceedings of the National Academy of Sciences of the United States of America*, *102*(23), 8245–8250. https://doi.org/10.1073/pnas.0409902102

Wang, H., Liu, H., Cao, G., Ma, Z., Li, Y., Zhang, F., Zhao, X., Zhao, X., Jiang, L., Sanders, N. J., Classen, A. T., He, J. S., & Liu, L. (2020). Alpine grassland plants grow earlier and faster but biomass remains unchanged over 35 years of climate change. *Ecology Letters*, *23*(4), 701–710. https://doi.org/10.1111/ele.13474

Xu, C., Liu, H., Williams, A. P., Yin, Y., & Wu, X. (2016). Trends toward an earlier peak of the growing season in northern hemisphere mid-latitudes. *Global Change Biology*, *22*(8), 2852–2860. https://doi.org/10.1111/gcb.13224

Yamori, W., Hikosaka, K., & Way, D. A. (2014). Temperature response of photosynthesis in C3, C4, and CAM plants: Temperature acclimation and temperature adaptation. *Photosynthesis Research*, *119*, 101–117. https://doi.org/10.1007/s11120-013-9874-6

Yang, J., Dong, J., Xiao, X., Dai, J., Wu, C., Xia, J., Zhao, G., Zhao, M., Li, Z., Zhang, Y., & Ge, Q. (2019). Divergent shifts in peak photosynthesis timing of temperate and alpine grasslands in China. *Remote Sensing of Environment*, *233*, 111395. https://doi.org/10.1016/j.rse.2019.111395

Zellweger, F., de Frenne, P., Lenoir, J., Vangansbeke, P., Verheyen, K., Bernhardt-Römermann, M., Baeten, L., Hédl, R., Berki, I., Brunet, J., van Calster, H., Chudomelová, M., Decocq, G., Dirnböck, T., Durak, T., Heinken, T., Jaroszewicz, B., Kopecký, M., Máliš, F., … Coomes, D. (2020). Forest microclimate dynamics drive plant responses to warming. *Science*, *368*, 772–775. https://doi.org/10.1126/science.aba6880

SUPPORTING INFORMATION

Additional supporting information can be found online in the Supporting Information section at the end of this article.

How to cite this article: Wang, B., Chen, W., Tian, D., Li, Z., Wang, J., Fu, Z., Luo, Y., Piao, S., Yu, G., & Niu, S. (2023). Dryness limits vegetation pace to cope with temperature change in warm regions. *Global Change Biology*, *29*, 4750–4757. https://doi.org/10.1111/gcb.16842